Development 129, 3455-3468 (2002)
Printed in Great Britain © The Company of Biologists Limited 2002
DEV3662

The Foxh1-dependent autoregulatory enhancer controls the level of Nodal signals in the mouse embryo

Dominic P. Norris*, Jane Brennan, Elizabeth K. Bikoff and Elizabeth J. Robertson†

Department of Molecular and Cellular Biology, Harvard University, The Biological Laboratories, Cambridge, MA 02138, USA
*Present address: Medical Research Council Mammalian Genetics Unit, Harwell OX11 0RD, UK
†Author for correspondence (e-mail: ejrobert@fas.harvard.edu)

Accepted 12 April 2002

SUMMARY

The TGFβ-related growth factor Nodal governs anteroposterior (AP) and left-right (LR) axis formation in the vertebrate embryo. A conserved intronic enhancer (ASE), containing binding sites for the fork head transcription factor Foxh1, modulates dynamic patterns of *Nodal* expression during early mouse development. This enhancer is responsible for early activation of *Nodal* expression in the epiblast and visceral endoderm, and at later stages governs asymmetric expression during LR axis formation. We demonstrate ASE activity is strictly Foxh1 dependent. Loss of this autoregulatory enhancer eliminates transcription in the visceral endoderm and decreases *Nodal* expression in the epiblast, but causes surprisingly discrete developmental abnormalities. Thus lowering the level of Nodal signaling in the epiblast disrupts both orientation of the AP axis and specification of the definitive endoderm. Targeted removal of the ASE also dramatically reduces left-sided *Nodal* expression, but the early events controlling LR axis specification are correctly initiated. However loss of the ASE disrupts *Lefty2* (*Leftb*) expression and causes delayed *Pitx2* expression leading to late onset, relatively minor LR patterning defects. The feedback loop is thus essential for maintenance of Nodal signals that selectively regulate target gene expression in a temporally and spatially controlled fashion in the mouse embryo.

Key words: Mouse, Nodal, Axis specification, Foxh1

INTRODUCTION

The Nodal signaling pathway plays fundamental roles during early development of all vertebrates (reviewed by Schier and Shen, 2000; Whitman, 2001). In the mouse, Nodal is required for initial specification of the anteroposterior (AP) axis (Brennan et al., 2001), mesoderm formation (Zhou et al., 1993; Conlon et al., 1994) and left-right (LR) patterning (Collignon et al., 1996; Lowe et al., 1996). Similarly, in zebrafish embryos, the *Nodal* homologs *cyclops* and *squint* control the development of head and trunk mesoderm and endodermal tissues (Feldman et al., 2000), and in *Xenopus Nodal*-related molecules act as mesoderm inducers (Jones et al., 1995). Recent studies in both *Xenopus* and zebrafish demonstrate the strength of Nodal signals determines cell fate. Thus, low levels of expression are sufficient to induce mesoderm, while high levels of expression are required for the development of endodermal cell lineages (Agius et al., 2000; Gritsman et al., 2000). These important issues have proven difficult to address in mouse embryos because of reciprocal Nodal-dependent interactions between the epiblast and the extra-embryonic tissues (Brennan et al., 2001).

Nodal signals via the Alk4 or Alk7 type I receptor in association with either the ActRIIA or ActRIIB type II receptor (reviewed by Whitman, 2001). The activated receptor complex phosphorylates the intracellular molecules Smad2 and Smad3, which in turn associate with Smad4 (Massague et al., 2000) and translocate to the nucleus. Cooperatively with other DNA-binding proteins, Smad proteins regulate transcription of target genes (reviewed by Wotton and Massague, 2001). Studies of activin responsive promoters in *Xenopus* have identified two Smad2/4-interacting DNA partners. The forkhead domain protein Foxh1 (formerly known as FAST1/2) binds as part of a complex to the activin responsive element of the *Mix2* gene (Chen et al., 1996; Chen et al., 1997). Similarly members of the Mix family of homeodomain proteins, in association with Smad2/4, activate the *Gsc* promoter (Germain et al., 2000). Loss of *Foxh1* function in mouse results in a range of developmental defects broadly consistent with a role in mediating Nodal signals (Hoodless et al., 2001; Yamamoto et al., 2001). *Foxh1* is not required for mesoderm formation, but mutant embryos show AP axis patterning defects, as well as abnormal development of the node and definitive endoderm, both of which are derivatives of the anterior primitive streak. Similarly, zebrafish *schmalspur* (*Foxh1* homolog) loss-of-function mutant embryos lack axial mesendoderm (Boggetti et al., 2000; Pogoda et al., 2000; Sirotkin et al., 2000). These defects are considerably less severe than those resulting from loss of Nodal function (Zhou et al., 1993; Conlon et al., 1994), suggesting that Nodal activates target genes required for initial axis specification and mesoderm formation via Foxh1-independent pathways.

Nodal expression is tightly regulated in a highly dynamic fashion at discrete tissue sites during early mouse development (Collignon et al., 1996; Varlet et al., 1997). *Nodal* mRNA is first detected throughout the epiblast and overlying visceral endoderm (VE). As development proceeds, *Nodal* is confined to the prospective posterior epiblast, marking the site of primitive streak formation. *Nodal* is lost from the VE after the onset of gastrulation, and becomes progressively down-regulated in the primitive streak. In the node, *Nodal* transcripts appear in a discrete population of cells located on the edges of the ventrally located notochordal plate, and become more strongly expressed on the left. At later stages *Nodal* is induced in a broad stripe of left lateral plate mesoderm (LPM). Mutations that disturb asymmetric *Nodal* expression inevitably cause defective LR axis patterning (Collignon et al., 1996; Lowe et al., 1996). Similarly, *Nodal* mis-expression in chick, fish or *Xenopus* embryos reverses the orientation of the LR body axis (reviewed by Capdevila et al., 2000).

Transgenic approaches have been used to map *cis*-regulatory elements responsible for spatially and temporally restricted *Nodal* expression patterns (Adachi et al., 1999; Norris and Robertson, 1999; Brennan et al., 2001) (D. P. N. and E. J. R., unpublished). An intronic enhancer, termed the ASE, controls early expression in the epiblast and VE, and also at later stages on the left side of the embryo. The minimal ASE enhancer region contains two *Foxh1*-binding sites (Saijoh et al., 2000). Similar *Foxh1*-dependent regulatory elements control asymmetric *Lefty2* (*Leftb* – Mouse Genome Informatics) and *Pitx2* expression (Saijoh et al., 1999; Shiratori et al., 2001). Moreover, *Foxh1*-dependent *cis*-acting regulatory elements have been mapped within the *Nodal* locus of all vertebrates examined (reviewed by Whitman, 2001). We have used gene targeting techniques to delete the ASE and test its role in axial patterning. The developmental abnormalities seen in *trans*-heterozygous embryos carrying the ASE deletion and a null allele ($Nodal^{\Delta 600/-}$), and homozygous mutant embryos ($Nodal^{\Delta 600/\Delta 600}$) were compared. In $Nodal^{\Delta 600/-}$ embryos, *Nodal* is expressed at low levels in the early epiblast and becomes confined to proximal epiblast cells; however, expression is undetectable in the VE. Reduced *Nodal* expression levels are sufficient for formation of the anterior visceral endoderm (AVE) and mesoderm induction. Many of these embryos, however, incorrectly position the AP axis, leading to abnormal gastrulation and cell movements. Moreover, $Nodal^{\Delta 600/-}$ embryos lack anterior definitive endoderm (ADE) and display rostral CNS patterning defects. By contrast, in homozygous $Nodal^{\Delta 600/\Delta 600}$ embryos, *Nodal* is more efficiently expressed in the epiblast but absent from the VE. Unexpectedly, these embryos develop normal AP pattern. Later, at early somite stages, *Nodal* expression in the LPM is significantly reduced, leading to failure to activate *Lefty2*, delayed activation of *Pitx2* and defective LR axis patterning. Overall, we conclude the *Foxh1*-dependent autoregulatory enhancer maintains and amplifies Nodal signals that selectively activate target genes responsible for patterning the embryonic body plan.

MATERIALS AND METHODS

Gene targeting

$Nodal^{LacZ/+}$ ES cells were transfected with the Δ600 targeting construct (Norris and Robertson, 1999) and selected in Hygromycin B. DNA prepared from individual drug-resistant colonies was genotyped by Southern blot analysis, as previously described (Norris and Robertson, 1999). After identification of targeted clones, the selection cassette was removed by transient expression of Cre recombinase and colonies isolated by low density plating. Approximately one in 15 of the drug-resistant clones were targeted with equivalent recombination frequencies on both chromosomes. Targeting events and removal of the hygromycin selection cassette were confirmed using 5′ and 3′ probes. Selected ES cell lines were used to generate germline chimeric mice that were subsequently bred to ICR females (Taconic).

Mouse breeding and genotyping

$Nodal^{LacZ}$, $Nodal^{\Delta 100.lacZ}$, $Nodal^{\Delta 600.LacZ}$ and transgenic lines expressing *lacZ* were PCR genotyped for the presence of the *lacZ* gene. Δ600 mice were genotyped by PCR using Δ600-5 (5′ GCT AGT GGC GCG ATC GGA ATG GA 3′) and Δ600-6 (5′ AAG GGA AGT GAA CTG GAA AGG TAT GT 3′): a 350 bp fragment shows presence of the deletion; a 950 bp fragment shows the wild-type allele. *Foxh1* mutant mice were a kind gift from Jeff Wrana and Pamela Hoodless, and were genotyped according to published protocols (Hoodless et al., 2001). All strains used in this analysis were maintained by breeding to ICR mice (Taconic).

WISH and histology

Whole-mount in situ hybridization was performed according to standard procedures. Probes for the following genes were used in this study: α cardiac actin (Roebroek et al., 1998), *Bmp4* (Winnier et al., 1995), *cripto* (Ding et al., 1998), *Eomes* (Russ et al., 2000), *Foxa2* (previously known as Hnf3β) (Sasaki and Hogan, 1996), *Gsc* (Blum et al., 1992), *Hex* (Thomas et al., 1998), *Lefty* (*Ebaf* – Mouse Genome Informatics) (Meno et al., 1996), *Lhx1* (Barnes et al., 1994), *Nodal* (Conlon et al., 1994), *Otx2* (Ang et al., 1994), *Pitx2* (Ryan et al., 1998), *Shh* (Echelard et al., 1993), *T* (Herrmann, 1991) and *Wnt3* (Liu et al., 1999). For histology embryos were fixed in 4% paraformaldehyde (PFA), dehydrated through an ethanol series and embedded in wax before sectioning. Hematoxylin and Eosin staining and X-gal staining were performed according to standard protocols. India ink was injected into the left ventricle of embryos at 14.5 dpc and 18.5 dpc, and allowed to fill the ventricle. Whether or not the ink moved directly into the right ventricle was scored visually.

RESULTS

Foxh1 regulates activity of the ASE but not the posterior epiblast enhancer (PEE)

The ASE, which is responsible for early *Nodal* expression in the VE and epiblast and at later stages asymmetric expression in LPM (Adachi et al., 1999; Norris and Robertson, 1999), is thought to be regulated by the forkhead transcription factor *Foxh1* (Saijoh et al., 2000). Deletion of the 100 bp core region containing the two *Foxh1*-binding sites causes striking changes to the expression of a $Nodal^{LacZ}$ reporter allele (Norris and Robertson, 1999). Thus *lacZ* activity was restricted to the proximal epiblast, absent from the VE and severely attenuated in the LPM of $Nodal^{\Delta 100.lacZ/+}$ embryos. To demonstrate directly that *Foxh1* modulates *Nodal* activity via associations with the ASE, we examined ASE-*lacZ* transgene expression in *Foxh1* mutant embryos (Hoodless et al., 2001). In wild-type embryos at early post-implantation stages, the transgene is active throughout the epiblast and VE, but expression becomes localized to the prospective posterior

prior to the initiation of gastrulation (Fig. 1B) (Norris and Robertson, 1999). In striking contrast, expression is undetectable in *Foxh1*$^{-/-}$ embryos (Fig. 1C). To test whether Foxh1 is sufficient for activation of the ASE, we removed the entire 600 bp ASE (Fig. 1A). The resulting *Nodal*$^{\Delta 600.LacZ}$ allele is expressed proximally but not distally in the epiblast (Fig. 1E,G) due to the activity of the 5′ posterior epiblast enhancer (PEE) (Norris and Robertson, 1999; Brennan et al., 2001) (D. P. N. and E. J. R., unpublished). Similar *Nodal*$^{\Delta 600.LacZ}$ expression patterns were observed in a *Foxh1*$^{-/-}$ background (Fig. 1H), confirming the Foxh1-independent activity of the PEE. A proportion of *Foxh1*$^{-/-}$ *Nodal*$^{+/-}$ mutant embryos were previously shown to display more severe patterning defects than *Foxh1*$^{-/-}$ embryos (Yamamoto et al., 2001). Similarly, here some (~25%) of *Foxh1*$^{-/-}$ *Nodal*$^{\Delta 600.LacZ}$ and *Foxh1*$^{-/-}$ *Nodal*$^{LacZ/+}$ mutant embryos express *lacZ* throughout the epiblast (Fig. 1F, 1I). Interestingly, this expanded *Nodal* expression domain and the associated morphological disturbances closely resemble those observed for Smad2 mutant embryos (Waldrip et al., 1998).

Reduced Nodal expression in Nodal$^{\Delta 600/-}$ embryos disrupts PD axis rotation

To examine ASE function in vivo, we deleted the 600 bp enhancer in the context of the wild-type locus (Fig. 1A). At day 6.5, the majority of *Nodal*$^{\Delta 600/-}$ embryos (60%) are indistinguishable from wild type (Table 1). However, the remaining 40% develop abnormally and display a characteristic morphology (Fig. 2A). In these overtly abnormal *Nodal*$^{\Delta 600/-}$ embryos, gastrulation is initiated and mesoderm induced radially around the proximal epiblast. These embryos also have a thickened patch of visceral endoderm characteristic of the AVE (Kimura et al., 2000) located at or just lateral to the distal tip of the epiblast, suggesting that the AVE forms normally but fails to rotate, as is the case for *Otx2* and cripto mutants (Ding et al., 1998; Perea-Gomez et al., 2001). These embryos also display a marked constriction at the embryonic/extra-embryonic boundary (Fig. 2B,C), and as gastrulation proceeds, the pro-amniotic canal often becomes constricted, resulting in the formation of two separate cavities (Fig. 2B,C).

To assess tissue disturbances further, we analyzed a panel of molecular markers. In the overtly abnormal *Nodal*$^{\Delta 600/-}$ embryos, posterior epiblast markers such as cripto (Ding et al., 1998), T (Thomas et al., 1998) and Wnt3 (Liu et al., 1999) are ectopically expressed throughout proximal regions of the epiblast (Fig. 2B-D). Occasionally, T-positive cells corresponding to proximal nascent mesoderm were found in the extra-embryonic region (Fig. 2C; also observed for *Nodal*^{LacZ} expression in Fig. 3C). This cell population lacks expression of the epiblast marker *Pou5f1* (formerly *Oct4*), and thus represents mesodermal cells migrating into the yolk sac (data not shown). Collectively these results demonstrate that mesoderm induction occurs throughout the proximal epiblast in *Nodal*$^{\Delta 600/-}$ embryos. *Foxa2* (formerly *Hnf3β*) is initially expressed throughout the VE, but by 6.5dpc localizes to the AVE and the anterior primitive streak (Perea-Gomez et al., 1999) (Fig. 2E). In mutant *Nodal*$^{\Delta 600/-}$ embryos, *Foxa2* transcripts are found at the proximal and distal most extent of the embryonic region, suggesting the proximal distal axis is formed correctly but fails to rotate. Additional AVE markers, including *Hex* (Thomas et al., 1998) and *Lhx1* (Perea-Gomez et al., 1999) gave similar results (Fig. 2F,G). Expression of the extra-embryonic markers *Eomes* and *Bmp4* is unperturbed in *Nodal*$^{\Delta 600/-}$ embryos (Fig. 2J,K). We also examined expression of *Gsc* and *Lefty1*, putative targets of *Nodal*/*Foxh1* signaling (Labbe et al., 1998; Yamamoto et al., 2001). *Gsc* normally marks the AVE and the anterior primitive streak; however, in mutant embryos, expression is markedly reduced and in some cases the AVE expression domain is entirely absent (Fig. 2H). Using a cross-reactive probe (Meno et al., 1997) that detects both *Lefty1* and *Lefty2* (Fig. 2I), we found *Lefty2* expressed in the nascent mesoderm, but *Lefty1* fails to be induced in the VE of *Nodal*$^{\Delta 600/-}$ embryos. Thus, we observe a distinctive perturbation of AP axis position in a high proportion of *Nodal*$^{\Delta 600/-}$ embryos.

Next, we analyzed *Nodal* mRNA expression patterns. As shown in Fig. 3A, *lacZ* expression is undetectable in the distal epiblast of *Nodal*$^{\Delta 600.LacZ/+}$ embryos. Similarly in *Nodal*$^{\Delta 600/-}$ embryos reduced levels of *Nodal* mRNA are confined to the proximal epiblast (Fig. 3B). This reduced level, however, is

Table 1. Summary of mutant phenotypes

(A) Recovery of phenotypically abnormal embryos from *Nodal*$^{\Delta 600/+}$×*Nodal*$^{-/+}$ crosses

Age (dpc)	Total number of embryos	Number of mutants	Number of embryos resorbed	Percentage of mutants
6.5	67	6	1	9.0*
7.5	56	14	2	25
8.5	262	54	5	20
9.5	23	3	1	13
10.5	8	2	-	25
12.5	12	0	1	-

Proportion of *Nodal*$^{\Delta 600/-}$ embryos showing overt mutant phenotype (as described in the text).

*At 6.5dpc 9% of embryos show thickened VE at the distal tip, representing 36% (6/17) of the expected number of mutant embryos.

(B) Proportion of *Nodal*$^{\Delta 600/+}$ embryos excluded from the yolk sac

Age (dpc)	Number of mutants	In VYS*	Excluded from VYS
7.5	14	7 (50%)	7 (50%)
8.5	54	32 (59%)	22 (41%)

*Embryos entirely contained within the VYS (visceral yolk sac).

(C) Recovery of mutants from *Nodal*$^{\Delta 600/+}$ intercrosses

Age	Total number	Wild type	Heterozygous mutant	Homozygous mutant	Percentage of mutants
14.5 dpc	54	12	29	13*	24
18.5 dpc	62			10	16
1 dpp	24	6	15	3	12.5
3/4 dpp	24	6	16	2	8.5
1 week	27	9	16	2	7.5
2 weeks					
3-4 weeks	25	6	16	3	12
5+ weeks	128	42	83	3†	2.5

*Seven had two left lung lobes, six had three left lung lobes.

†Three animals were genotyped, but died before they could be examined. One corpse was recovered and showed right pulmonary isomerism and an enlarged heart.

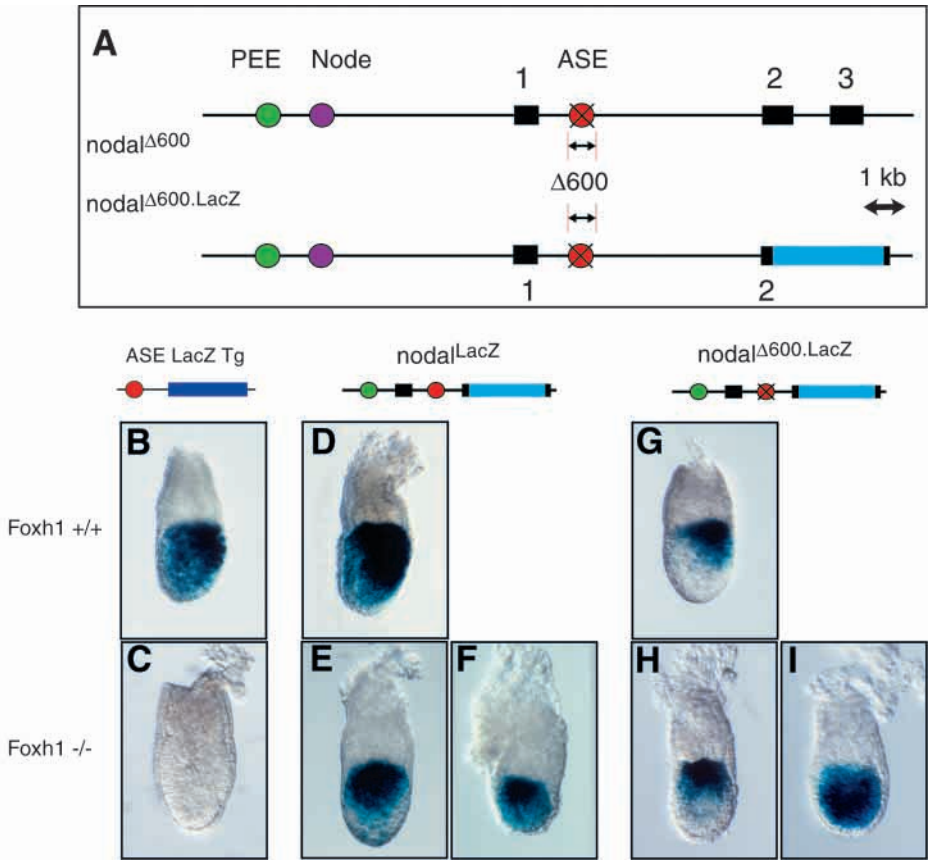

Fig. 1. *Foxh1* is essential for ASE activity in vivo. (A) The Δ600 ASE deletion was engineered in the context of both the wild-type and *Nodal*^{LacZ} loci, resulting in the *Nodal*$^{\Delta 600}$ and *Nodal*$^{\Delta 600.LacZ}$ alleles, as indicated. The PEE, Node and ASE enhancers are indicated by colored circles, and the exons by black boxes. (B-I) β-Galactosidase staining patterns in 6.5 dpc embryos with anterior towards the left. (B) Wild-type (WT) embryos express the ASE *lacZ* transgene in the epiblast (more strongly in the posterior than the anterior) and overlying VE. (C) By contrast, the ASE *lacZ* transgene is not expressed in *Foxh1*-deficient embryos. (D) *Nodal*^{LacZ} is expressed in the epiblast and overlying VE of WT embryos. By contrast, in *Foxh1*-deficient embryos (E), expression is proximally restricted within the epiblast and lost from the overlying VE. (F) A proportion (25%) of *Foxh1*$^{-/-}$, *Nodal*$^{LacZ/+}$ embryos show a more severe phenotype, are rounded in appearance with a uniformly thickened VE, and display β-galactosidase staining throughout the epiblast but not in the VE. (G) *Nodal*$^{\Delta 600.LacZ/+}$ embryo showing expression confined to the proximal posterior epiblast, and undetectable in the VE. (H) In *Foxh1*$^{-/-}$ embryos, *Nodal*$^{\Delta 600.LacZ}$ expression is similarly restricted to the proximal epiblast but lacks AP asymmetry. (I) A rare *Foxh1*$^{-/-}$, *Nodal*$^{\Delta 600.LacZ/+}$ embryo, with a more severe phenotype showing β-galactosidase staining throughout the epiblast. PEE, posterior epiblast element; ASE, asymmetric element; Node, node-specific enhancer.

sufficient to activate expression in the VE, as evidenced by the pattern of X-gal staining in the VE of *Nodal*$^{\Delta 600/LacZ}$ embryos (Fig. 3C). By contrast, the VE of *Nodal*$^{\Delta 600.LacZ/\Delta 600.LacZ}$ embryos fails to express *lacZ* (Fig. 3D). Thus, activation of *Nodal* in the VE requires Foxh1/Smad2 associations with the autoregulatory ASE.

Failure to specify anterior definitive endoderm in *Nodal*$^{\Delta 600/-}$ embryos

While only 40% of *Nodal*$^{\Delta 600/-}$ embryos exhibit overt morphological defects at early gastrulation stages, by 7.5 dpc, all *Nodal*$^{\Delta 600/-}$ embryos are distinctly abnormal (Table 1). As mentioned above, approximately 40% exhibit a visible constriction at the embryonic/extra-embryonic boundary at 6.5 dpc, which varies in severity ranging from a slightly noticeable narrowing to almost complete separation of these regions (Fig. 4A,B; summarized in Table 1). Slightly later at 8.5 dpc, this class of most severely disturbed embryos develop external to the visceral yolk sac (VYS) (Fig. 4E). In some cases, the anterior regions are partially externalized, while the primitive streak is retained within the VYS (Fig. 4D). Histological analysis demonstrates the presence of neural tissue (Fig. 4D,E), but midline tissues are largely absent resulting in fused somites (data not shown). This is likely to be due to defective gastrulation movements that secondarily lead to abnormal node morphogenesis and failure to form a notochord. Cells expressing the myocardial marker α cardiac actin are juxtaposed to the VYS in severely affected embryos (data not shown), suggesting that cardiac precursors are specified normally.

The majority of mutant embryos develop within the VYS, exhibit a normal midline, somites and yolk-sac morphology (Fig. 4C), but have defective cardiac looping (data not shown). By 8.5 dpc, *Nodal*$^{\Delta 600/-}$ embryos begin to display a marked reduction in anterior neural tissues. As the AVE is correctly specified, and the node and notochord form normally, these developmental abnormalities probably result from defective formation of the anterior definitive endoderm (ADE), a tissue arising from the anterior streak that is known to be responsible for patterning the CNS (Martinez Barbera et al., 2000). In keeping with this conclusion, Hex expression, a marker of definitive endoderm, is not detected in *Nodal*$^{\Delta 600/-}$ embryos from gastrulation stages onwards (data not shown). Expression of *Shh*, a marker of ADE, is punctate and highly downregulated even in grossly normal *Nodal*$^{\Delta 600/-}$ embryos (Fig. 4F). The anterior *Shh* domain normally extends into the ventral forebrain by 8.5 dpc (Fig. 4G,H), but in *Nodal*$^{\Delta 600/-}$ mutant embryos, expression is truncated at the hindbrain (arrowhead in Fig. 4G). The most severely affected *Nodal*$^{\Delta 600/-}$ embryos also display decreased midline tissue and deficiencies in definitive endoderm formation (Fig. 4I). Similar data were obtained analyzing *Foxa2* (Fig. 4J,K). *Nodal*$^{\Delta 600/-}$ embryos also display reduced expression of *Otx2* (Fig. 4L,M), a marker of forebrain tissue (Ang et al., 1994).

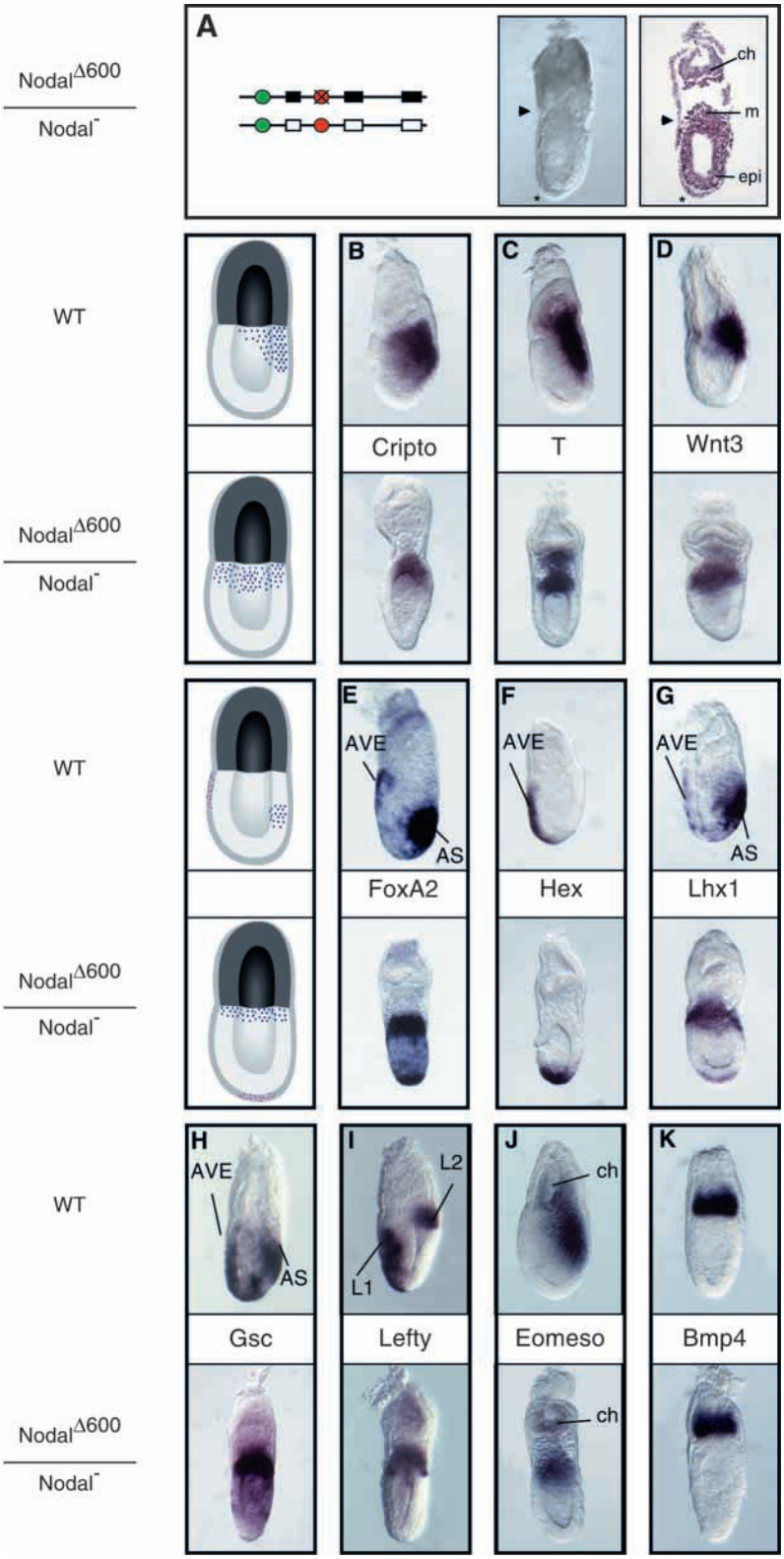

Fig. 2. Defective PD to AP rotation in *Nodal*$^{\Delta 600/-}$ embryos. Primitive streak (B-D,F-I), AVE (E-I) and extra-embryonic ectoderm (K,J) marker analysis in 6.5 dpc embryos. Wild-type controls are shown above *Nodal*$^{\Delta 600/-}$mutants. Cartoons indicate primitive streak/mesoderm markers in blue and AVE markers in pink. Anterior is towards the left. (A) *Nodal*$^{\Delta 600/-}$ embryo. Mesoderm (m) is visible proximal to the epiblast (epi), while the chorion (ch) is proximally displaced. The VE shows a distinct thickening at the distal tip (indicated by *). The embryonic/extra-embryonic boundary is indicated by the arrowhead. (B) Cripto, which is normally localized to the posterior epiblast, is expressed throughout the proximal epiblast. (C) *T* (brachyury) marks the nascent mesoderm and primitive streak. In *Nodal*$^{\Delta 600/-}$ mutant embryos, *T* is expressed symmetrically in the proximal epiblast and in the extra-embryonic mesoderm. (D) *Wnt3*, which is normally confined to the posterior proximal epiblast and overlying VE just prior to and following the initiation of gastrulation, is expressed symmetrically throughout the proximal epiblast in *Nodal*$^{\Delta 600/-}$ mutant embryos, but is absent from the VE (data not shown). (E) *Foxa2* is expressed in the anterior primitive streak (AS) and the AVE. In *Nodal*$^{\Delta 600/-}$ mutant embryos, *Foxa2* is expressed in distal VE and epiblast. (F) *Hex* is expressed in the AVE both prior to and following the initiation of gastrulation in wild-type embryos. *Hex* is also expressed in newly formed definitive endoderm (DE) by mid streak stages. *Hex* expression in *Nodal*$^{\Delta 600/-}$ mutant embryos is restricted to the distal most VE. (G) *Lhx1* is expressed in mesoderm emerging from the anterior primitive streak (AS) and in the AVE at gastrulation, but in *Nodal*$^{\Delta 600/-}$ mutant embryos expression is present in the proximal epiblast and the distal VE. (H) Goosecoid (*Gsc*), a putative target of *Nodal* signaling, is expressed in AVE and anterior primitive streak. In *Nodal*$^{\Delta 600/-}$ mutant embryos, *Gsc* expression is only weakly detected in the proximal epiblast and the distal VE in a proportion of embryos and is undetectable in others. (I) *Lefty1* and *Lefty2* expression, examined using a common in situ hybridization probe that detects both transcripts, shows that *Lefty1* (L1) is expressed in the AVE, and *Lefty2* (L2) in nascent mesoderm. In *Nodal*$^{\Delta 600/-}$ mutant embryos, *Lefty1* expression in the AVE is not detected. *Lefty2* expression is detected in the proximal epiblast of mutant embryos. (J) The T box gene eomesodermin (*Eomes*) is expressed in the chorion (ch) and the posterior epiblast. In *Nodal*$^{\Delta 600/-}$ mutant embryos, expression is maintained in the chorion, while epiblast expression is proximal. (K) Expression of *Bmp4*, which marks extra-embryonic ectoderm, is unaffected in *Nodal*$^{\Delta 600/-}$ embryos.

Because a normal notochord is present in the majority of *Nodal*$^{\Delta 600/-}$ embryos, specification of the node, a derivative of the anterior streak, appears to be relatively unaffected. Thus, *Nodal* expression controlled by the 5′ node element (Norris and Robertson, 1999), which remains intact in the *Nodal*$^{\Delta 600}$ allele, is sufficient to promote node morphogenesis.

AP and LR patterning in *Nodal*$^{\Delta 600/\Delta 600}$ embryos

As shown in Fig. 5, in contrast to *Nodal*$^{\Delta 600/-}$ embryos, we

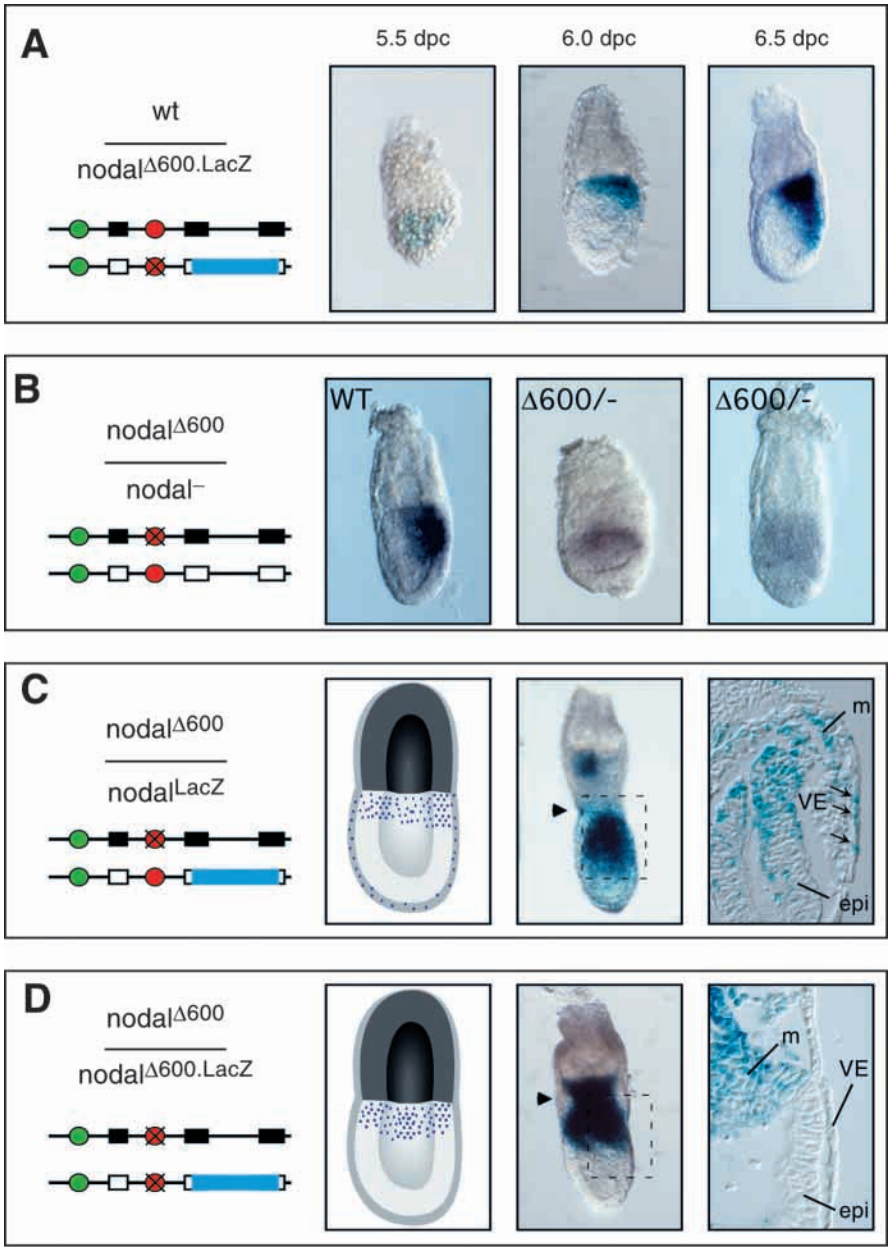

Fig. 3. Disturbed *Nodal* expression patterns in *Nodal*$^{\Delta 600/-}$ embryos. Genotypes are indicated towards the left of each panel. Black boxes indicate functional *Nodal* alleles and null alleles are shown as white boxes. The blue box represents the *lacZ* insertion into exon 2 of *Nodal*. Enhancers are indicated as circles, the PEE in green and the ASE in red. The Δ600 deletion is indicated by the cross. In all panels, anterior is towards the left. (A) As assessed by β-gal staining, punctate *Nodal*$^{\Delta 600.LacZ}$ expression observed at 5.5 dpc throughout the epiblast becomes restricted to the proximal epiblast by 6.5 dpc and gradually resolves to the posterior. Expression continues in the primitive streak after the onset of gastrulation, but is undetectable in the VE. (B) *Nodal* expression directly assessed by whole-mount in situ hybridization. In contrast to wild type (WT), expression in *Nodal*$^{\Delta 600/-}$ embryos is noticeably reduced, restricted to the proximal epiblast, and fails to show obvious AP asymmetry. Section analysis confirms the loss of expression within the VE (data not shown). (C) *Nodal* expression in *Nodal*$^{LacZ/\Delta 600}$ embryos is proximally restricted. The embryo shows a characteristic constriction at the embryonic/extra-embryonic boundary (arrowhead). The position of the section shown is indicated by the box. β-Gal staining is clearly detectable in the VE of these embryos (arrows). (D) β-Gal staining and tissue morphology in *Nodal*$^{\Delta 600.LacZ/\Delta 600}$ embryos resemble that in C. Arrowhead indicates embryonic/extra-embryonic boundary. However no *lacZ* expression is detected in the VE. VE, visceral endoderm; m, mesoderm; epi, epiblast.

found that *Nodal*$^{\Delta 600/\Delta 600}$ embryos efficiently undergo AVE rotation, display a correctly positioned primitive streak, and gastrulate normally. In comparison with *Nodal*$^{\Delta 600/-}$ embryos, *Nodal* expression within the epiblast is elevated roughly twofold in *Nodal*$^{\Delta 600/\Delta 600}$ homozygous mutants. This increased dose is sufficient to rescue ADE formation and axis patterning defects. *Nodal* mRNA is expressed at significantly reduced levels in the epiblast, and is undetectable in the VE (Fig. 5A-D). Thus, *Nodal* expression within the VE is not essential for either specification or positioning of the AVE. Rather, these processes depend on the strength of Nodal signals within the epiblast. At 7.5 and 8.5 dpc, expression within the node closely resembles that in wild type (Fig. 5E,F), except that asymmetry of expression is lost. Later, at early somite stages, *Nodal*$^{\Delta 600/\Delta 600}$ embryos display only weak *Nodal* expression in LPM (Fig. 5J-L), although invariably on the left side of the axis.

By the eight-somite stage, *Nodal*$^{\Delta 600/\Delta 600}$ embryos exhibit abnormal heart looping morphogenesis (Fig. 6). To evaluate the onset of LR patterning defects, we assessed expression of downstream targets, including the homeodomain protein *Pitx2* and the *Nodal* antagonists *Lefty2* and *Lefty1* (Saijoh et al., 2000; Shiratori et al., 2001). Lefty 2 expression is normally downregulated concomitantly with that of *Nodal* (Meno et al., 1996). Only a few *Nodal*$^{\Delta 600/\Delta 600}$ embryos (30%) express *Lefty2* transcripts (Fig. 6B). As shown in Fig. 6A, *Lefty1* is asymmetrically expressed in the prospective floorplate of the neural tube, whereas in *Nodal*$^{\Delta 600/\Delta 600}$ embryos *Lefty1* is missing from the midline and only weakly expressed in a few cells close to the node (Fig. 6B).

Pitx2 mutant embryos exhibit right sided lung isomerisms, abnormal cardiac morphogenesis, reduced spleen development and incomplete turning (Gage et al., 1999; Kitamura et al.,

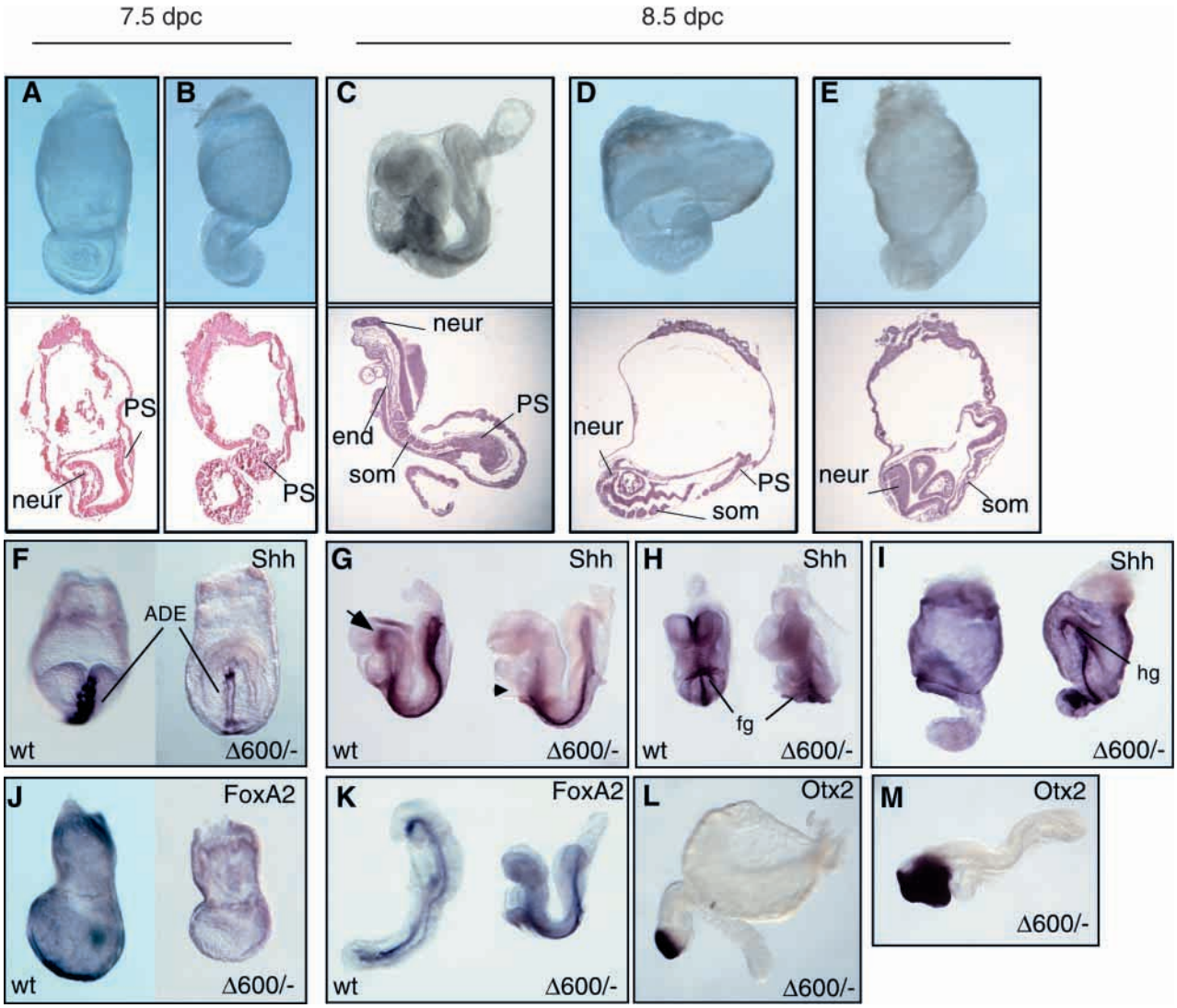

Fig. 4. *Nodal* signals are required for definitive endoderm specification. (A-E) *Nodal*$^{\Delta 600/-}$ mutant embryos at 7.5 dpc (A,B) and 8.5 dpc (C-E). Hematoxylin and Eosin stained sections of the embryos are shown in the bottom of each panel. Two classes of embryo are apparent by 7.5 dpc (Table 1); those that gastrulate inside the visceral yolk sac (VYS) (A), and those that gastrulate externally (B). Twenty-four hours later, embryos remaining inside the VYS form an AP axis, but show defects in heart looping and anterior truncations (C). Embryos that grow external to the VYS develop an AP axis with somites along the trunk; however, fused somites indicate the midline may be defective in many embryos. The posterior is closely associated with the VYS in approximately half of these embryos (D), and in the others both the anterior and posterior are fully external to the VYS (E). end, endoderm; neur, neurectoderm; PS, primitive streak; som, somite. (F-M) Whole-mount in situ hybridization of 7.5 dpc (F,J) and 8.5 dpc (G-I,K-M) embryos. Anterior views (F,H) and lateral views with anterior towards the left (G,I-M). (F) Sonic hedgehog (*Shh*) is expressed in the midline anterior definitive endoderm (ADE) of WT embryos. *Nodal*$^{\Delta 600/-}$ mutant embryos show highly reduced *Shh* expression. (G) One day later, *Shh* expression in the midline extends into the ventral forebrain in the WT embryo (arrow); however, this expression domain is absent in *Nodal*$^{\Delta 600/-}$ mutant embryos. The anterior extent of the expression is indicated by the arrowhead. (H) Anterior view of the embryos shown in G, underscoring the absence of ventral forebrain expression and greatly reduced anterior foregut (fg) expression domain in the *Nodal*$^{\Delta 600/-}$ mutant embryo. (I) In severely affected *Nodal*$^{\Delta 600/-}$ mutant embryos, *Shh* expression is confined to the posterior midline. The embryo on the right expresses *Shh* along the length of the midline and in hindgut endoderm (hg). There is no obvious anterior gut endoderm population in either embryo. (J) *Foxa2* is expressed in the node, midline and ADE in the WT embryo, but is highly downregulated in *Nodal*$^{\Delta 600/-}$ mutant embryos at a similar stage. (K) Later in development, *Foxa2* expression in the CNS and ADE extends into the ventral forebrain of the WT embryo. By contrast, *Foxa2* expression is restricted to the level of heart (indicated by arrowhead) in *Nodal*$^{\Delta 600/-}$ mutants. (L,M) *Nodal*$^{\Delta 600/-}$ mutant embryos stained with *Otx2* to assess the presence of forebrain/midbrain tissue. A severely affected embryo (L) and an embryo with the less severe phenotype (M) both express *Otx2* in a distinct, but highly reduced, anterior domain.

1999; Lin et al., 1999; Lu et al., 1999). Low levels of *Pitx2* are required for specification of atrial situs and increased expression is necessary for establishment of lung situs (Gage et al., 1999; Kitamura et al., 1999; Liu et al., 2001). *Pitx2* transcription is initiated in left LPM coincident with the onset of asymmetric *Nodal* expression. We found the onset of asymmetric *Pitx2* expression is slightly delayed in *Nodal*$^{\Delta 600/\Delta 600}$ embryos and becomes visible only at the five-

to six-somite stage (Fig. 6D). Moreover, the anterior extent of the *Pitx2* expression domain is markedly reduced by the eight- to 10-somite stage (Fig. 6E,F). At 9.5 dpc, *Pitx2* expression normally extends behind the sinoatrial region of the heart, but in *Nodal*$^{\Delta 600/\Delta 600}$ embryos the anterior extent of expression is reduced by approximately one to two somite widths (Fig. 6G,H).

To analyze embryonic turning and establishment of organ situs, *Nodal*$^{\Delta 600/\Delta 600}$ embryos were allowed to develop beyond 8.5 dpc. At early somite stages, none of a large panel of mutant embryos showed morphological defects (Table 1). However, by 9.0 dpc, heart looping is visibly abnormal in *Nodal*$^{\Delta 600/\Delta 600}$ embryos, with the heart positioned more ventrally than in wild type (Fig. 7A,B). The heart tubes appear to fold normally, suggesting they have acquired regional patterning. Moreover, heart contractions and blood circulation develop normally (data not shown). By 11.5 dpc, mutant hearts display an ambiguously positioned apex (Fig. 7C). In addition, the lungs of mutant embryos display lobation defects (Fig. 7C; Table 1). Differences in branching morphogenesis normally leads to the formation of four lobes on the right and a single lobe on the left side of the thoracic cavity. By contrast, *Nodal*$^{\Delta 600/\Delta 600}$ embryos develop partial right isomerisms (Fig. 7C).

LR patterning not only affects heart and lung morphogenesis, but is also essential for establishment of the correct connection of the heart to the vasculature (Kathiriya and Srivastava, 2000). Defects in the aortic arches (Fig. 7D-G) were assessed visually and by India ink injections. The aortic arch normally exits the left ventricle, behind the pulmonary artery, and arches to the right; three arteries branch upwards delivering blood to the upper body (Fig. 7D). The pulmonary artery exits the right ventricle arches to the right and splits into two arteries that lead to the lungs. Prenatally, however, the pulmonary artery empties through the ductus ateriosus into the dorsal aorta. In *Nodal*$^{\Delta 600/\Delta 600}$ embryos an enlarged aorta rises in front of the pulmonary

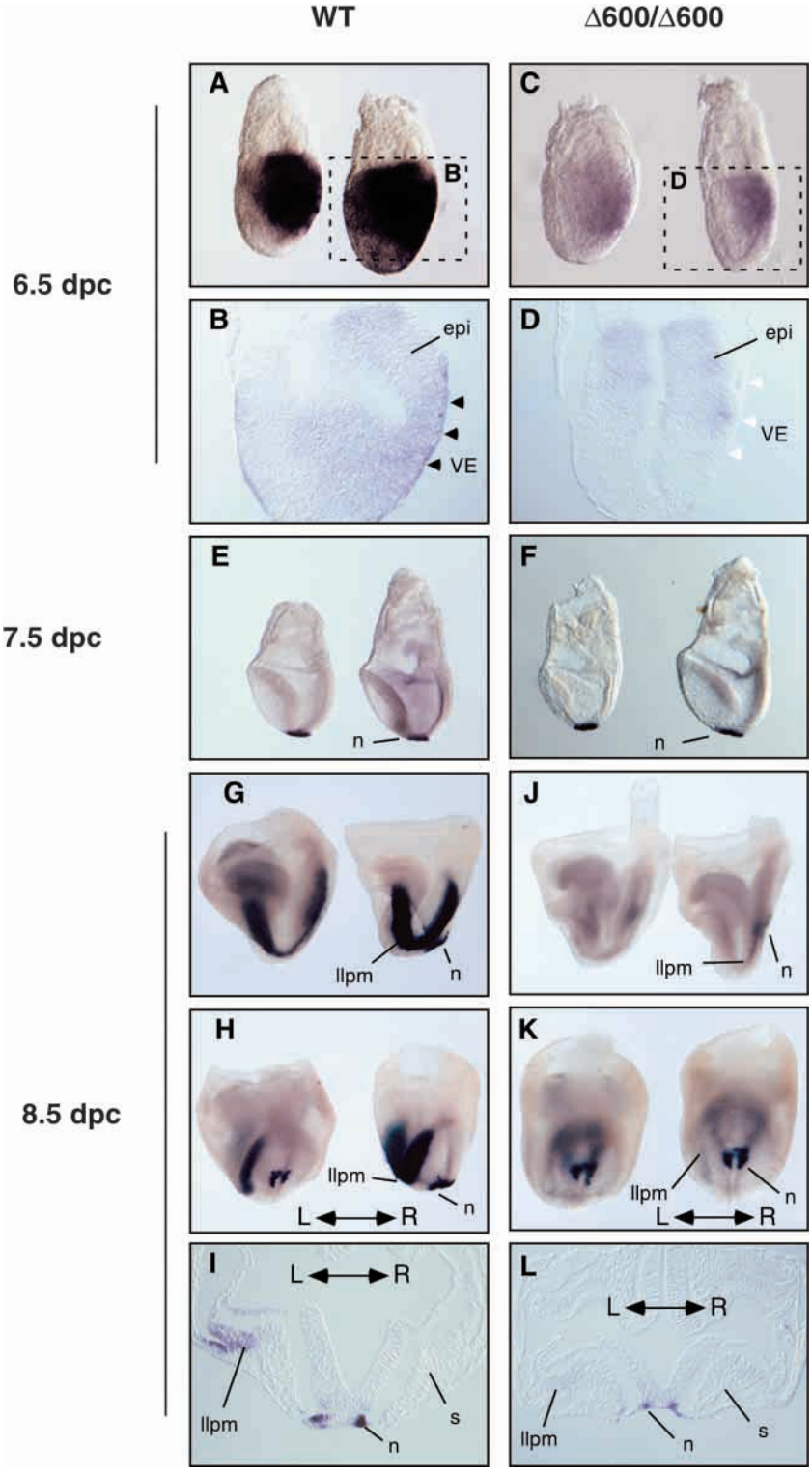

Fig. 5. Normal AP patterning and endoderm specification in *Nodal*$^{\Delta 600/\Delta 600}$ embryos. (A) Whole-mount analysis of endogenous *Nodal* mRNA expression in WT embryos at 6.5 dpc. The box indicates the position of the sagittal section shown in B. (B) *Nodal* expression in the epiblast (epi) and visceral endoderm (VE) is indicated by black arrowheads. (C) *Nodal* $^{\Delta 600/\Delta 600}$ mutants show markedly reduced expression within the epiblast. (D) Sagittal section shows loss of expression within the VE (white arrowheads). (E) In WT embryos at 7.5 dpc, *Nodal* mRNA is confined to the node (n). (F) *Nodal* $^{\Delta 600/\Delta 600}$ mutants are morphologically indistinguishable from WT and display robust *Nodal* expression in the node. (G) Asymmetric *Nodal* expression in the node and left lateral plate mesoderm (llpm) of WT embryos at 8.5 dpc. (H) Posterior views of embryos shown in G. (I) Transverse section shows asymmetric *Nodal* expression. (J) *Nodal* $^{\Delta 600/\Delta 600}$ mutant embryos strongly express *Nodal* in the node. A proportion of embryos exhibit a very low level of expression in the left LPM. Posterior view (K) and section (L) of the *Nodal* $^{\Delta 600/\Delta 600}$ mutant embryo shown on the right in J, confirming node expression is equivalent on both sides. s, somite. All panels are lateral views with anterior towards left, except H and K, which show posterior views.

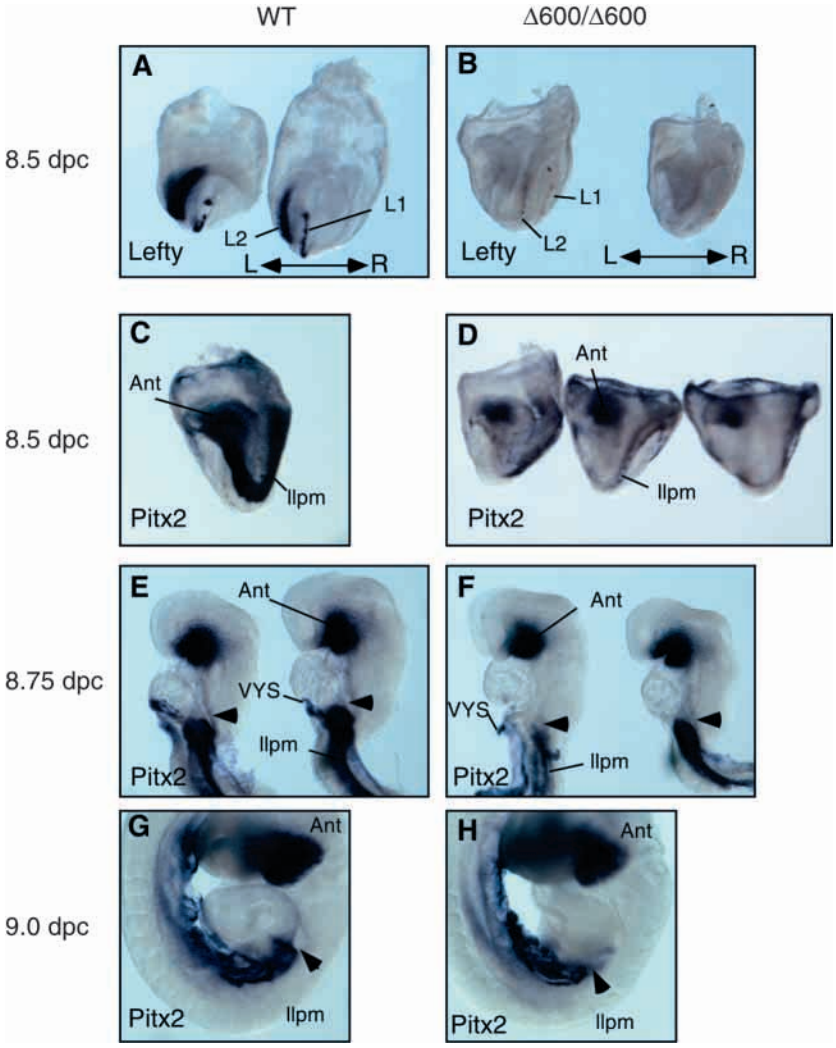

Fig. 6. Loss of Lefty gene expression and delayed activation of *Pitx2* activation in *Nodal*$^{\Delta 600/\Delta 600}$ embryos. Whole-mount in situ analysis of *Lefty1* (L1) and *Lefty2* (L2) (using a common lefty probe; A,B) and *Pitx2* (C-H) in *Nodal*$^{\Delta 600/\Delta 600}$ embryos (B,D,F,H) and wild-type controls (A,C,E,G). Lateral views with anterior towards left, except for A (posterior view). (A) *Lefty1* expression on the left side of the prospective floorplate of the neural tube and *Lefty2* in the left LPM in wild-type embryos. (B) *Lefty1* is not expressed in *Nodal*$^{\Delta 600/\Delta 600}$ mutants, except in a few midline cells close to the node. *Lefty2* is expressed in ~30% of mutant embryos but at significantly lower levels (left-hand embryo in B). (C) *Pitx2* expression in the head and left lateral plate mesoderm (llpm) from the three-somite stage in WT embryos. (D) *Nodal*$^{\Delta 600/\Delta 600}$ mutant embryos maintain the anterior expression domain seen in WT embryos, but have a reduced level of expression in the llpm. Note the llpm expression is more posteriorly restricted compared with that in WT. (E) At 8.75 dpc, asymmetric *Pitx2* expression in the llpm extends behind the sinoatrial region of the heart (anterior extent of expression indicated by arrowheads). Remnants of the visceral yolk sac (VYS) expressing *Pitx2* are seen lateral to the llpm. (F) The anterior extent of *Pitx2* expression in the llpm is posteriorly restricted in *Nodal*$^{\Delta 600/\Delta 600}$ mutant embryos and is absent from tissue lying behind the sinoatrial region of the heart (arrowheads). (G) After embryonic turning, the difference in the anterior extent of llpm expression of *Pitx2* is particularly obvious (compare positions of arrowheads in G and H). The expression in the *Nodal*$^{\Delta 600/\Delta 600}$ mutant embryos (H) is anteriorly restricted by approx. two somite widths compared with the wild type (G). This results in *Pitx2* not being expressed behind the sinoatrial region of the heart in the mutants. Aberrant heart looping is also obvious within this mutant embryo, although the direction of embryonic turning is normal. Ant, anterior.

artery (Fig. 7F,G), giving rise to four ascending arteries. The pulmonary artery empties into the descending aorta through the ductus ateriosus (Fig. 7G). Moreover, ink injected into the right ventricle immediately filled the left ventricle implicating ventriculoseptal defects (data not shown). Approximately 30% of *Nodal*$^{\Delta 600/\Delta 600}$ embryos survive to birth (Table 1). However, these are often runted, and none survives beyond 6 weeks of age.

DISCUSSION

The Foxh1-dependent autoregulatory enhancer maintains and amplifies Nodal signals in vivo

Dynamic patterns of *Nodal* expression are tightly regulated during early mouse development (Collignon et al., 1996; Varlet et al., 1997). An intronic enhancer termed the ASE, which controls expression in the epiblast, VE and left lateral plate mesoderm contains two *Foxh1*-binding sites (Saijoh et al., 2000). Recent in vitro studies suggest that the range and intensity of Nodal signals are in part controlled by an autoregulatory feedback loop (reviewed by Whitman, 2001). The present experiments demonstrate ASE activity in mouse embryos is strictly Foxh1 dependent. Acting in an autocrine manner, the ASE maintains and amplifies *Nodal* transcription, and thereby increases the amount of ligand produced locally. The ASE also functions in a paracrine fashion to expand expression domains. Specifically, the ASE controls Nodal-dependent target gene expression in the VE. The *Foxh1*-dependent autoregulatory enhancer thus establishes a gradient of *Nodal* signals that is crucial for mesoderm induction, endoderm specification and AP and LR axis patterning during early mouse development (summarized in Fig. 8).

The strength of Nodal signals in the epiblast controls orientation of the AP axis

Shortly after implantation, at the egg cylinder stage, the mouse embryo exhibits a distinct molecular pattern along its proximodistal (PD) axis. The final AP axis is positioned by coordinated cell movements that rotate this pre-existing PD axis, and thus restrict mesoderm induction to the proximal posterior epiblast (reviewed by Beddington and Robertson, 1999; Lu et al., 2001). Nodal signals from the epiblast establish this PD pattern (Brennan et al., 2001). The ASE has an important role controlling *Nodal* activation in the VE and in

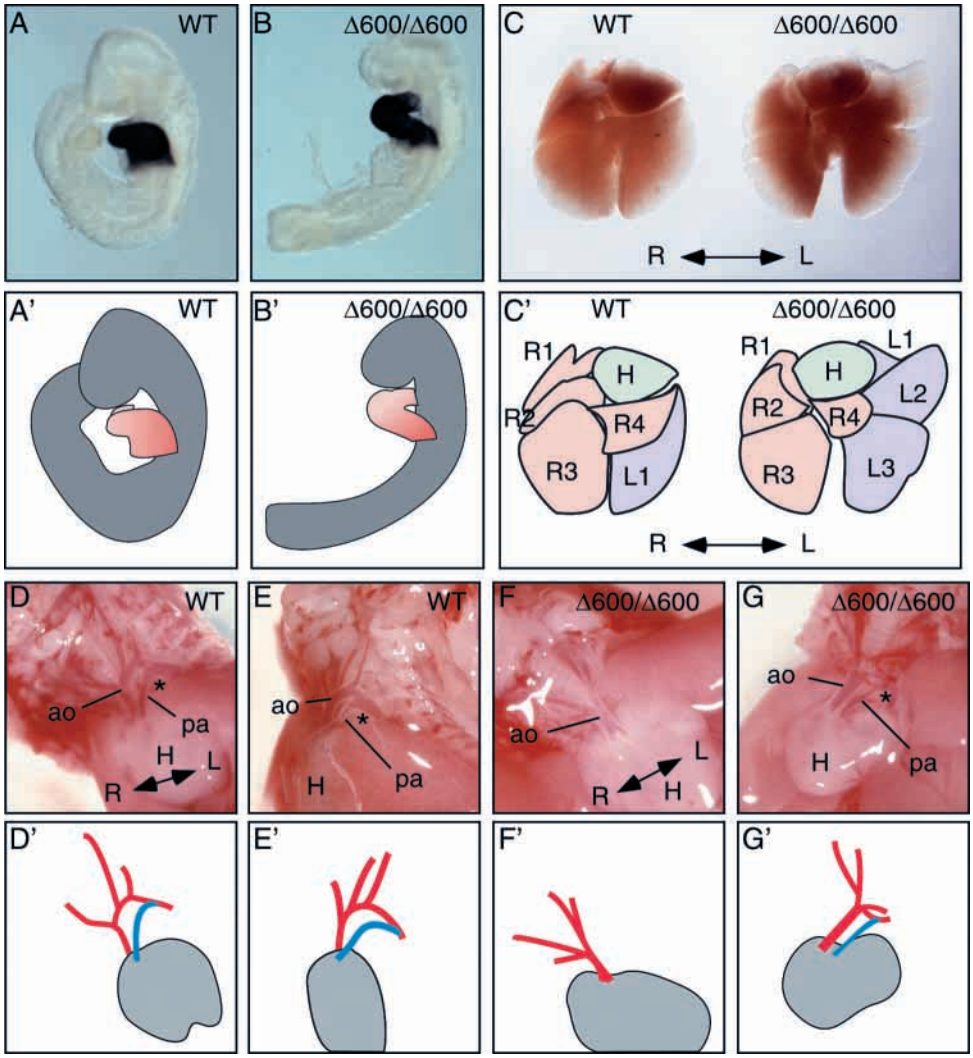

Fig. 7. *Nodal*$^{\Delta 600/\Delta 600}$ embryos exhibit heart and lung situs defects. In wild-type (WT) embryos at 9.5 dpc (A), the heart loops laterally across the body of the embryo, while in *Nodal*$^{\Delta 600/\Delta 600}$ mutant embryos (B), the heart loops ventrally. Hearts are visualized by expression of the myocardial marker α-cardiac actin. Looping differences are summarized in A' and B'. (C) In WT 12.5 dpc embryos (left), the lungs branch to give four lobes on the right and one lobe on the left. By contrast, *Nodal*$^{\Delta 600/\Delta 600}$ mutant embryos (right) have four right lobes and two or three left lobes, indicating partial right isomerism. In WT embryos, the apex of the heart (H) points to the left, while in mutant embryos it is more medially positioned. These differences are summarized in the cartoon in C'. Lung lobes are labeled R1, 2, 3 and 4 to indicate the cranial, middle, caudal and accessory lobes, respectively, and L1, 2 and 3 to indicate the normal left lobe or duplicated cranial lobe (L1), the duplicated middle lobe (L2) and the duplicated caudal lobe (L3). Hearts from WT (D,E) and *Nodal*$^{\Delta 600/\Delta 600}$ mutant (F,G) embryos collected ~12 hours before birth. The thoracic cavity has been dissected away to reveal the heart and the major blood vessels leading from it. The view is from the ventral side of the embryo in D and F, and of the same embryos rotated onto their right sides in E and G. In all panels, rostral is upwards. (D) WT heart. The aorta (ao) emerges from behind the pulmonary artery (pa) and arches to the left. The subclavian and common carotid arteries ascend from the aortic arch. The pulmonary artery emerges form the heart and at this stage of development empties through the ductus arteriosus (indicated by *) into the aorta. The left and right pulmonary arteries that deliver blood to the lungs carry very little blood prior to birth and are not visible in these embryos. (E) View of embryo in D from the left hand side. The pulmonary artery (pa) can be clearly seen to emerge from in front of the aorta (ao). (F) *Nodal*$^{\Delta 600/\Delta 600}$ mutant embryo. A large aorta (ao) is present in this embryo that divides into four ascending vessels. The pulmonary artery is not visible from this angle lying directly behind aorta. (G) View of embryo in F from the left-hand side. In addition to the aorta, from this angle it is possible to see the pulmonary artery (pa) that empties into the aorta through the ductus arteriosus (indicated by *). (D'-G') Schematics of D-G, indicting the position of the aortic arch and ascending arteries in red and the pulmonary artery in blue.

amplifying *Nodal* signaling in the epiblast. At day 5.5, *Nodal* expression is initiated throughout the epiblast of *Nodal*$^{\Delta 600/-}$ embryos, but in contrast to wild type, expression rapidly becomes confined only to proximal epiblast cells. Thus, ASE activity maintains widespread expression in a broader domain of the epiblast, and activates *Nodal* transcription in the VE. These results demonstrate that *Nodal* mRNA expression, as assessed by whole-mount in situ hybridization, is greatly reduced in the absence of the feedback loop. Nonetheless, the low levels of *Nodal* expression in the epiblast of *Nodal*$^{\Delta 600/-}$ embryos are sufficient for establishment of correct PD pattern, and promote expression of genes such as *Wnt3* and *Eomes*, which are required for mesoderm formation. *Nodal*$^{\Delta 600/-}$ embryos also maintain expression of *Bmp4* in the adjacent extra-embryonic ectoderm, and markers of the AVE such as Hex are induced in the overlying VE. In a high percentage of *Nodal*$^{\Delta 600/-}$ embryos, the PD axis is imprecisely converted to AP pattern, a phenotype also seen in embryos homozygous for a hypomorphic *Nodal* allele (Lowe et al., 2001). Because the AP axis is rescued in *Nodal*$^{\Delta 600/\Delta 600}$ embryos, we conclude that this defect reflects decreased levels of *Nodal* signaling in the epiblast. Thus, *Nodal* transcription is initiated via upstream regulatory elements, probably the PEE. In *Nodal*$^{\Delta 600/-}$ embryos, Nodal activity is sufficient to induce mesoderm formation, but insufficient to promote cell movements that position the AP axis. Loss of the *Nodal* co-factor cripto causes similar patterning defects (Ding et al., 1998), suggesting that the strength of Nodal ligand/receptor interactions in the epiblast controls cell growth and/or morphogenetic movements.

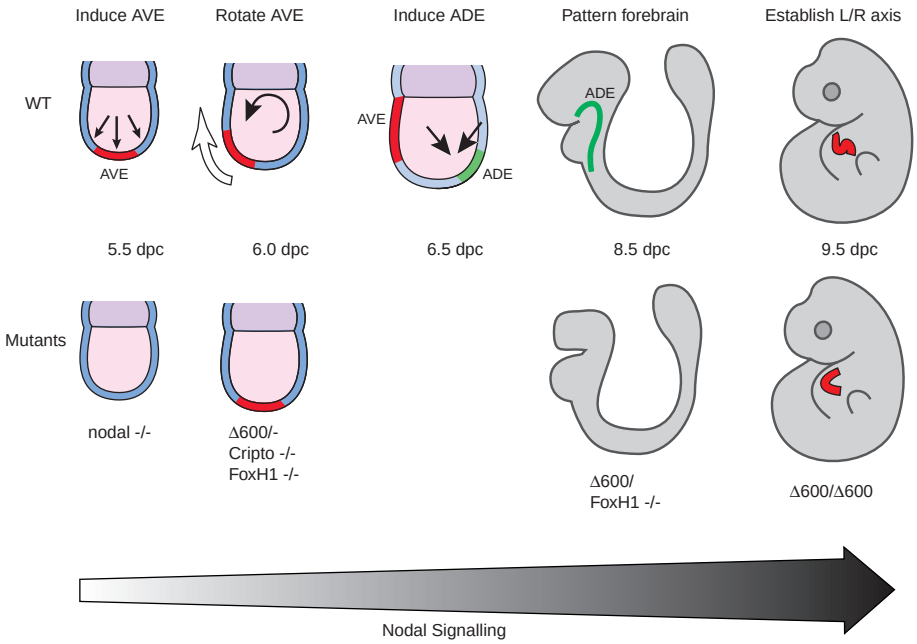

Fig. 8. An autoregulatory feedback loop controls dosage dependent *Nodal* signals responsible for embryonic patterning. *Nodal* null embryos fail to induce an AVE at 5.5dpc. *Cripto*-null, and some $Nodal^{\Delta 600/-}$ and $Foxh1^{-/-}$ embryos induce but fail to rotate the AVE at 6.0 dpc, owing to lowered *Nodal* signaling. Other $Nodal^{\Delta 600/-}$, and $Foxh1^{-/-}$ embryos rotate the AVE but fail to induce the ADE at 6.5 dpc, resulting in reduction of the forebrain at 8.5 dpc. $Nodal^{\Delta 600/\Delta 600}$ embryos have yet higher level of *Nodal* signaling and correctly induce and rotate the AVE and induce the ADE at 6.5 dpc, yet they fail to establish the LR axis correctly at 8.5 dpc, resulting in defects in heart looping visible at 9.5 dpc.

Nodal expression in visceral endoderm is not required for anterior patterning

Embryos that lack the ASE fail to express *Nodal* mRNA in the VE. Thus, activation of the *Nodal* locus in the VE is strictly controlled by the *Smad2*/*Foxh1*-dependent pathway. However, markers of the AVE are activated normally in $Nodal^{\Delta 600/-}$ embryos. Thus, Nodal signals within the VE are nonessential for early anterior patterning. Consistent with this, embryos deficient in *Foxh1*, and therefore lacking Nodal activity in the VE, also establish a normal AVE (Hoodless et al., 2001; Yamamoto et al., 2001). An interesting feature of $Nodal^{\Delta 600/-}$ embryos is that they develop a severe physical constriction at the extra-embryonic/embryonic boundary that subsequently leads to externalization and growth of the embryo outside of the yolk sac. Similar defects have been described for *Foxa2* and *Lhx1* mutants (Ang and Rossant, 1994; Shawlot and Behringer, 1995). In the case of *Foxa2*, this probably reflects a requirement for Foxa2 within the VE, as the defect is not seen in chimeric embryos in which the VE is wild type (Dufort et al., 1998). Loss of *Foxh1* also results in VE constriction, and this defect is also alleviated in mutant embryos in which the VE is wild type (Yamamoto et al., 2001). By contrast, $Nodal^{\Delta 600/\Delta 600}$ embryos that lack Nodal activity in the VE develop normally. The morphological defects in $Nodal^{\Delta 600/-}$ embryos are therefore most likely due to decreased Nodal signaling from the epiblast that in turn attenuates expression of downstream target genes acting in the VE. In keeping with this idea, we find that expression of genes such as *Gsc* and *Lefty1*, which represent downstream targets of the *Nodal* pathway (Labbe et al., 1998; Yamamoto et al., 2001), are induced poorly, if at all, in $Nodal^{\Delta 600/-}$ embryos. We conclude that the strength of Nodal signaling from the epiblast is crucial in controlling activation of discrete *Nodal* targets in the VE that in turn are responsible for normal growth and morphogenesis of the VE.

Nodal signals control formation of the definitive gut endoderm

Interestingly $Foxh1^{-/-}$ (Hoodless et al., 2001; Yamamoto et al., 2001) and $Nodal^{\Delta 600/-}$ embryos both develop anterior CNS truncations, a phenotype similar to that which develops in chimeric embryos lacking *Nodal* function in the VE (Varlet et al., 1997). Here, by contrast, we observe normal development of $Nodal^{\Delta 600/\Delta 600}$ embryos, arguing that Nodal is not required in the VE. Similarly *Foxh1*, while essential for *Nodal* activation in the VE, is not required for formation of the AVE (Hoodless et al., 2001; Yamamoto et al., 2001). The current findings suggest an alternative explanation for the development of these anterior defects, namely that lowering the dose of Nodal signaling in the epiblast, either genetically or via cell mixing in chimeras, leads to a failure to correctly specify definitive endoderm tissue. The definitive endoderm (DE) initially appears as a discrete cell layer at the most distal end of the primitive streak (Lawson et al., 1986; Lawson and Pedersen, 1987; Kinder et al., 2001), displacing primitive visceral endoderm into the extra-embryonic regions (Lawson and Pedersen, 1987; Tam and Beddington, 1992; Thomas and Beddington, 1996). Recent evidence has shown that the signals provided by the anterior gut endoderm are essential for reinforcing and correctly elaborating pattern in the developing neural plate after displacement of the AVE. Thus, embryos lacking the transcription factor *Hex* fail to form anterior definitive endoderm and develop anterior CNS truncations (Martinez Barbera et al., 2000). Similarly, the Wnt inhibitor Dkk-1 acting in the anterior mesendoderm (Mukhopadhyay et al., 2001), and the pro-protein convertase SPC4 expressed in the foregut (Constam and Robertson, 2000) are both required for patterning of the rostral CNS. Our current findings indicate in mouse, as for *Xenopus* (Agius et al., 2000), that Nodal signaling is essential for specification of the definitive endoderm lineage.

Neither *Foxh1* (Hoodless et al., 2001) nor *Smad2* (Tremblay et al., 2000) -deficient ES cells are competent to form definitive

endoderm, suggesting Foxh1/Smad2 complexes govern endodermal fate in the anterior streak. Chimeras composed of *Nodal*-deficient VE, with *Nodal* expression only partially restored in the epiblast, phenocopy $Nodal^{\Delta 600/-}$ embryos (Varlet et al., 1997). Thus, decreasing Smad2 signals in the anterior streak is sufficient to disrupt formation of DE, in turn leading to cardiac and anterior CNS defects. By contrast, in $Nodal^{\Delta 600/\Delta 600}$ embryos, increased levels of Nodal activity allow normal specification of the definitive endoderm lineage. Collectively, these findings establish a dose-dependent requirement for the *Nodal* signaling pathway in eliciting endodermal fates in the mouse.

Attenuated Nodal signals in the absence of the feedback loop cause relatively mild late onset LR patterning defects

Conserved *Nodal* activities are known to be essential for specification of the LR body axis (reviewed by Capdevila et al., 2000). Asymmetric activation of *Nodal* expression in the left lateral plate mesoderm at early somite stages in turn activates the downstream targets *Lefty2* and *Pitx2* (reviewed by Capdevila et al., 2000) and enhances *Nodal* transcription via the *Foxh1*-dependent autoregulatory enhancer. Deletion of the *Nodal* ASE enhancer severely compromises this pathway, and only low levels of asymmetric *Nodal* expression are transiently detected in $Nodal^{\Delta 600/\Delta 600}$ embryos.

Asymmetric *Lefty2* transcription is also mediated by an enhancer containing two *Foxh1*-binding motifs (Saijoh et al., 1999; Saijoh et al., 2000). Deletion of these sequences in the mouse germline results in failure to activate asymmetric *Lefty2* expression and causes ectopic *Nodal* expression leading to situs defects (Meno et al., 2001). $Nodal^{\Delta 600/\Delta 600}$ embryos either fail or only weakly activate *Lefty2* expression. *Lefty2* target gene expression thus requires continuous Nodal signaling. In addition, we found that *Lefty1*, which is normally expressed in the midline prospective floorplate tissue, is only rarely induced in $Nodal^{\Delta 600/\Delta 600}$embryos. These results implicate *Lefty1* as a downstream target. However, as yet, *Nodal* responsive cis-acting elements such as *Foxh1*-binding sites have not been identified at the *Lefty1* locus (Saijoh et al., 1999).

By contrast, decreased Nodal activity in $Nodal^{\Delta 600/\Delta 600}$ embryos is sufficient to activate robust *Pitx2* expression. Recent experiments have described a *Pitx2* transcriptional enhancer containing three *Foxh1*-binding motifs. In contrast to *Nodal*, *Pitx2* transcription is maintained via the activity of an *Nkx2.1*-dependent enhancer (Shiratori et al., 2001). The increased number or distinct configuration of the *Foxh1*-binding sites may allow *Pitx2* occupancy by activated Smad2/3/4 complexes transiently formed in $Nodal^{\Delta 600/\Delta 600}$ embryos. Nonetheless delayed activation of *Pitx2* transcription in the LPM results from the markedly reduced *Nodal* expression, that correlates with the development of right pulmonary isomerisms and heart defects in $Nodal^{\Delta 600/\Delta 600}$ embryos. As *Pitx2*-deficient embryos show similar thoracic defects (Gage et al., 1999; Kitamura et al., 1999; Lin et al., 1999; Lu et al., 1999), these abnormalities probably reflect altered *Pitx2* expression patterns.

Cryptic, a *Nodal* co-factor (Yan et al., 1999), and *Gdf1*, a TGFβ family member (Rankin et al., 2000), are both essential for asymmetric activation of *Nodal*, *Lefty2* and *Pitx2*. Loss-of-function mutants display right pulmonary isomerism and randomization of cardiac and abdominal situs, associated with randomization in the direction of embryonic turning and heart looping. Surprisingly, we found that dramatically decreasing Nodal activity in the lateral plate by elimination of the positive feedback loop had a relatively minor impact on LR patterning. Thus, the direction of embryonic turning or initial cardiac looping is unaffected in $Nodal^{\Delta 600/\Delta 600}$ embryos. This cannot be due to asymmetric activation of *Pitx2* in these embryos, as loss-of-function of *Pitx2* does not affect the direction of turning or prevent initial establishment of abdominal situs (Gage et al., 1999; Kitamura et al., 1999; Lin et al., 1999; Lu et al., 1999). Embryonic turning and abdominal situs may be therefore be controlled by distinct, *Nodal*-independent, molecular pathways. However, in chick (Logan et al., 1998; Piedra et al., 1998; Ryan et al., 1998) and *Xenopus* (Sampath et al., 1997; Ryan et al., 1998; Campione et al., 1999), ectopic *Nodal* expression can reverse body situs, suggesting that as yet undescribed *Nodal* targets may be activated to control this process. In this case, based on the phenotype of $Nodal^{\Delta 600/\Delta 600}$ embryos, only low levels of asymmetric Nodal activity are predicted to be required to activate these pathways.

It has been suggested that LR asymmetry is initiated in the mouse by a net leftward flow of extracellular fluid generated by the cilia located on the ventral surface of the node (reviewed by Capdevila et al., 2000). This asymmetric morphogen gradient is thought to act at a distance to induce asymmetric *Nodal* expression in the left lateral plate. Mutations affecting the formation or motility of the cilia disturb establishment of the asymmetric *Nodal* expression domain. Nodal ligand produced at the edge of the notochordal plate potentially represents this ‘morphogen’ and acts to induce its own transcription in the LPM. Consistent with this, recent work in zebrafish shows that the *Nodal* homolog *squint* can act at a distance (Chen and Schier, 2001). Similarly removal of the asymmetric expression domain of the *Nodal* antagonist *Lefty2*, results in bilateral *Nodal* expression, consistent with long range diffusion and autoactivation by secreted Nodal ligand (Meno et al., 2001).

However, the present findings challenge this simple model and allow us to draw two new conclusions about Nodal activities involved in establishing the LR axis. First, we demonstrate that asymmetric *Nodal* expression in the developing node is not essential to induce asymmetric *Nodal* transcription in the lateral plate, as $Nodal^{\Delta 600/\Delta 600}$ embryos express wild-type levels of *Nodal* transcripts in the node in a symmetric fashion, but *Nodal* is correctly induced exclusively on the left side of the axis. Thus, the functional significance of *Nodal* asymmetry in the mouse node remains unclear. Second, deletion of the autoregulatory enhancer fails to eliminate *Nodal* expression in the left LPM. Thus, tissue-specific activation of the locus occurs selectively on the left via an ASE- and probably Foxh1-independent mechanism(s). While key molecules controlling LR patterning have been identified in recent years, clearly additional work will be required to dissect the components of the functional pathways they control, and how they interact with each other to regulate this process.

We thank Jeff Wrana and Pamela Hoodless for providing the *Foxh1* mutant mice, Patti Lewko and Joe Rocca for animal care, Debbie Pelusi for genotyping assistance, Gerry Chu for advice about

histology, and Cindy Lu and Ray Dunn for comments on the manuscript. D. P. N. was supported by a Charles A King Trust Fellowship and J. B. by a Fellowship from the Wellcome Trust. This work was supported by a grant from the NIH to E. J. R.

REFERENCES

Adachi, H., Saijoh, Y., Mochida, K., Ohishi, S., Hashiguchi, H., Hirao, A. and Hamada, H. (1999). Determination of left/right asymmetric expression of nodal by a left side-specific enhancer with sequence similarity to a lefty-2 enhancer. *Genes Dev.* **13**, 1589-1600.

Agius, E., Oelgeschlager, M., Wessely, O., Kemp, C. and de Robertis, E. M. (2000). Endodermal Nodal-related signals and mesoderm induction in Xenopus. *Development* **127**, 1173-1183.

Ang, S. L., Conlon, R. A., Jin, O. and Rossant, J. (1994). Positive and negative signals from mesoderm regulate the expression of mouse Otx2 in ectoderm explants. *Development* **120**, 2979-2989.

Ang, S. L. and Rossant, J. (1994). HNF-3 beta is essential for node and notochord formation in mouse development. *Cell* **78**, 561-574.

Barnes, J. D., Crosby, J. L., Jones, C. M., Wright, C. V. and Hogan, B. L. M. (1994). Embryonic expression of Lim-1, the mouse homolog of Xenopus Xlim-1, suggests a role in lateral mesoderm differentiation and neurogenesis. *Dev. Biol.* **161**, 168-178.

Beddington, R. S. P. and Robertson, E. J. (1999). Axis development and early asymmetry in mammals. *Cell* **96**, 195-209.

Blum, M., Gaunt, S. J., Cho, K. W. Y., Steinbeisser, H., Blumberg, B., Bittner, D. and de Robertis, E. M. (1992). Gastrulation in the mouse: the role of the homeobox gene *goosecoid*. *Cell* **69**, 1097-1106.

Boggetti, B., Argenton, F., Haffter, P., Bianchi, M. E., Cotelli, F. and Beltrame, M. (2000). Cloning and expression pattern of a zebrafish homolog of forkhead activin signal transducer (FAST), a transcription factor mediating Nodal-related signals. *Mech. Dev.* **99**, 187-190.

Brennan, J., Lu, C. C., Norris, D. P., Rodriguez, T. A., Beddington, R. S. P. and Robertson, E. J. (2001). Nodal signalling in the epiblast patterns the early mouse embryo. *Nature* **411**, 965-969.

Campione, M., Steinbeisser, H., Schweickert, A., Deissler, K., van Bebber, F., Lowe, L. A., Nowotschin, S., Viebahn, C., Haffter, P., Kuehn, M. R. et al. (1999). The homeobox gene Pitx2: mediator of asymmetric left-right signaling in vertebrate heart and gut looping. *Development* **126**, 1225-1234.

Capdevila, J., Vogan, K. J., Tabin, C. J. and Izpisúa-Belmonte, J. C. (2000). Mechanisms of left-right determination in vertebrates. *Cell* **101**, 9-21.

Chen, X., Rubock, M. J. and Whitman, M. (1996). A transcriptional partner for MAD proteins in TGF-beta signalling. *Nature* **383**, 691-696.

Chen, X., Weisberg, E., Fridmacher, V., Watanabe, M., Naco, G. and Whitman, M. (1997). Smad4 and FAST-1 in the assembly of activin-responsive factor. *Nature* **389**, 85-89.

Chen, Y. and Schier, A. F. (2001). The zebrafish Nodal signal Squint functions as a morphogen. *Nature* **411**, 607-610.

Collignon, J., Varlet, I. and Robertson, E. J. (1996). Relationship between asymmetric nodal expression and the direction of embryonic turning. *Nature* **381**, 155-158.

Conlon, F. L., Lyons, K. M., Takaesu, N., Barth, K. S., Kispert, A., Herrmann, B. and Robertson, E. J. (1994). A primary requirement for *nodal* in the formation and maintenance of the primitive streak in the mouse. *Development* **120**, 1919-1928.

Constam, D. B. and Robertson, E. J. (2000). SPC4/PACE4 regulates a TGFbeta signaling network during axis formation. *Genes Dev.* **14**, 1146-1155.

Ding, J., Yang, L., Yam, Y.-T., Chen, A., Desai, N., Wynshaw-Boris, A. and Shen, M. M. (1998). *Cripto* is required for correct orientation of the anterior-posterior axis in the mouse embryo. *Nature* **395**, 702-707.

Dufort, D., Schwartz, L., Harpal, K. and Rossant, J. (1998). The transcription factor HNF3β is required for the visceral endoderm for normal primitive streak morphogensis. *Development* **125**, 3015-3025.

Echelard, Y., Epstein, D. J., St-Jacques, B., Shen, L., Mohler, J., McMahon, J. A. and McMahon, A. P. (1993). Sonic hedgehog, a member of a family of putative signaling molecules, is implicated in the regulation of CNS polarity. *Cell* **75**, 1417-1430.

Feldman, B., Dougan, S. T., Schier, A. F. and Talbot, W. S. (2000). Nodal-related signals establish mesendodermal fate and trunk neural identity in zebrafish. *Curr. Biol.* **10**, 531-534.

Gage, P. J., Suh, H. and Camper, S. A. (1999). Dosage requirement of Pitx2 for development of multiple organs. *Development* **126**, 4643-4651.

Germain, S., Howell, M., Esslemont, G. M. and Hill, C. S. (2000). Homeodomain and winged-helix transcription factors recruit activated Smads to distinct promoter elements via a common Smad interaction motif. *Genes Dev.* **14**, 435-451.

Gritsman, K., Talbot, W. S. and Schier, A. F. (2000). Nodal signaling patterns the organizer. *Development* **127**, 921-932.

Herrmann, B. G. (1991). Expression pattern of the Brachyury gene in whole-mount TWis/TWis mutant embryos. *Development* **113**, 913-917.

Hoodless, P. A., Pye, M., Chazaud, C., Labbe, E., Attisano, L., Rossant, J. and Wrana, J. L. (2001). FoxH1 (Fast) functions to specify the anterior primitive streak in the mouse. *Genes Dev.* **15**, 1257-1271.

Jones, C. M., Kuehn, M. R., Hogan, B. L., Smith, J. C. and Wright, C. V. (1995). Nodal-related signals induce axial mesoderm and dorsalize mesoderm during gastrulation. *Development* **121**, 3651-3662.

Kathiriya, I. S. and Srivastava, D. (2000). Left-right asymmetry and cardiac looping: implications for cardiac development and congenital heart disease. *Am. J. Med. Genet.* **97**, 271-279.

Kimura, C., Yoshinaga, K., Tian, E., Suzuki, M., Aizawa, S. and Matsuo, I. (2000). Visceral endoderm mediates forebrain development by suppressing posteriorizing signals. *Dev. Biol.* **225**, 304-321.

Kinder, S. J., Tsang, T. E., Wakamiya, M., Sasaki, H., Behringer, R. R., Nagy, A. and Tam, P. P. L. (2001). The organizer of the mouse gastrula is composed of a dynamic population of progenitor cells for the axial mesoderm. *Development* **128**, 3623-3634.

Kitamura, K., Miura, H., Miyagawa-Tomita, S., Yanazawa, M., Katoh-Fukui, Y., Suzuki, R., Ohuchi, H., Suehiro, A., Motegi, Y., Nakahara, Y. et al. (1999). Mouse Pitx2 deficiency leads to anomalies of the ventral body wall, heart, extra- and periocular mesoderm and right pulmonary isomerism. *Development* **126**, 5749-5758.

Labbe, E., Silvestri, C., Hoodless, P. A., Wrana, J. L. and Attisano, L. (1998). Smad2 and Smad3 positively and negatively regulated TGFβ-dependent transcription through the forkhead DNA-binding protein FAST2. *Mol. Cell* **2**, 109-120.

Lawson, K. A., Meneses, J. J. and Pedersen, R. A. (1986). Cell fate and cell lineage in the endoderm of the presomite mouse embryo, studied with an intracellular tracer. *Dev. Biol.* **115**, 325-339.

Lawson, K. A. and Pedersen, R. A. (1987). Cell fate, morphogenetic movement and population kinetics of embryonic endoderm at the time of germ layer formation in the mouse. *Development* **101**, 627-652.

Lin, C. R., Kioussi, C., O'Connell, S., Briata, P., Szeto, D., Liu, F., Izpisua-Belmonte, J. C. and Rosenfeld, M. G. (1999). Pitx2 regulates lung asymmetry, cardiac positioning and pituitary and tooth morphogenesis. *Nature* **401**, 279-282.

Liu, C., Liu, W., Lu, M. F., Brown, N. A. and Martin, J. F. (2001). Regulation of left-right asymmetry by thresholds of Pitx2c activity. *Development* **128**, 2039-2048.

Liu, P., Wakamiya, M., Shea, M. J., Albrecht, U., Behringer, R. R. and Bradley, A. (1999). Requirement for *Wnt3* in vertebrate axis formation. *Nat. Genet.* **22**, 361-365.

Logan, M., Pagan-Westphal, S. M., Smith, D. M., Paganessi, L. and Tabin, C. J. (1998). The transcription factor pitx2 mediates situs-specific morphogenesis in response to left-right asymmetric signals. *Cell* **94**, 307-317.

Lowe, L. A., Supp, D. M., Sampath, K., Yokoyama, T., Wright, C. V. E., Potter, S. S., Overbeek, P. and Kuehn, M. R. (1996). Conserved left-right asymmetry of nodal expression and alterations in murine *situs inversus*. *Nature* **381**, 158-161.

Lowe, L. A., Yamada, S. and Kuehn, M. R. (2001). Genetic dissection of nodal function in patterning the mouse embryo. *Development* **128**, 1831-1843.

Lu, C. C., Brennan, J. and Robertson, E. J. (2001). From fertilization to gastrulation: axis formation in the mouse embryo. *Curr. Opin. Genet. Dev.* **11**, 384-392.

Lu, M. F., Pressman, C., Dyer, R., Johnson, R. L. and Martin, J. F. (1999). Function of Rieger syndrome gene in left-right asymmetry and craniofacial development. *Nature* **401**, 276-278.

Martinez Barbera, J. P., Clements, M., Thomas, P., Rodriguez, T., Meloy, D., Kioussis, D. and Beddington, R. S. P. (2000). The homeobox gene Hex is required in definitive endodermal tissues for normal forebrain, liver and thyroid formation. *Development* **127**, 2433-2445.

Massague, J., Blain, S. W. and Lo, R. S. (2000). TGFbeta signaling in growth control, cancer, and heritable disorders. *Cell* **103**, 295-309.

Meno, C., Ito, Y., Saijoh, Y., Matsuda, Y., Tashiiro, K., Kuhara, S. and Hamada, H. (1997). Two closely related left-right asymmetrically expressed genes, lefty-1 and lefty-2: their distinct expression domains, chromosomal linkage and direct neuralizing activity in Xenopus embryos. *Genes Cells* **2**, 513-524.

Meno, C., Saijoh, Y., Fujii, H., Ikeda, M., Yokoyama, T., Yokoyama, M., Toyoda, Y. and Hamada, H. (1996). Left-right asymmetric expression of the TGFβ-family member *lefty* in mouse embryos. *Nature* **381**, 151-155.

Meno, C., Takeuchi, J., Sakuma, R., Koshiba-Takeuchi, K., Ohishi, S., Saijoh, Y., Miyazaki, J., ten Dijke, P., Ogura, T. and Hamada, H. (2001). Diffusion of nodal signaling activity in the absence of the feedback inhibitor lefty2. *Dev. Cell* **1**, 127-138.

Mukhopadhyay, M., Shtrom, S., Rodriguez-Esteban, C., Chen, L., Tsukui, T., Gomer, L., Dorward, D. W., Glinka, A., Grinberg, A., Huang, S. P. et al. (2001). Dickkopf1 is required for embryonic head induction and limb morphogenesis in the mouse. *Dev. Cell* **1**, 423-434.

Norris, D. P. and Robertson, E. J. (1999). Asymmetric and node-specific nodal expression patterns are controlled by two distinct cis-acting regulatory elements. *Genes Dev.* **13**, 1575-1588.

Perea-Gomez, A., Shawlot, W., Sasaki, H., Behringer, R. R. and Ang, S. (1999). HNF3beta and Lim1 interact in the visceral endoderm to regulate primitive streak formation and anterior-posterior polarity in the mouse embryo. *Development* **126**, 4499-4511.

Perea-Gomez, A., Lawson, K. A., Rhinn, M., Zakin, L., Brulet, P., Mazan, S. and Ang, S. L. (2001). Otx2 is required for visceral endoderm movement and for the restriction of posterior signals in the epiblast of the mouse embryo. *Development* **128**, 753-765.

Piedra, M. E., Icardo, J. M., Albajar, M., Rodriguez-Rey, J. C. and Ros, M. A. (1998). Pitx2 participates in the late phase of the pathway controlling left-right asymmetry. *Cell* **94**, 319-324.

Pogoda, H. M., Solnica-Krezel, L., Driever, W. and Meyer, D. (2000). The zebrafish forkhead transcription factor FoxH1/Fast1 is a modulator of nodal signaling required for organizer formation. *Curr. Biol.* **10**, 1041-1049.

Rankin, C. T., Bunton, T., Lawler, A. M. and Lee, S. J. (2000). Regulation of left-right patterning in mice by growth/differentiation factor-1. *Nat. Genet.* **24**, 262-265.

Roebroek, A. J., Umans, L., Pauli, I. G., Robertson, E. J., van Leuven, F., van de Ven, W. J. and Constam, D. B. (1998). Failure of ventral closure and axial rotation in embryos lacking the proprotein convertase Furin. *Development* **125**, 4863-4876.

Russ, A. P., Wattler, S., Colledge, W. H., Aparicio, S. A., Carlton, M. B., Pearce, J. J., Barton, S. C., Surani, M. A., Ryan, K., Nehls, M. C. et al. (2000). Eomesodermin is required for mouse trophoblast development and mesoderm formation. *Nature* **404**, 95-99.

Ryan, A. K., Blumberg, B., Rodriguez-Esteban, C., Yonei-Tamura, S., Tamura, K., Tsukui, T., de la Pena, J., Sabbagh, W., Greenwald, J., Choe, S. et al. (1998). Pitx2 determines left-right asymmetry of internal organs in vertebrates. *Nature* **394**, 545-551.

Saijoh, Y., Adachi, H., Mochida, K., Ohishi, S., Hirao, A. and Hamada, H. (1999). Distinct transcriptional regulatory mechanisms underlie left-right asymmetric expression of *lefty-1* and *lefty-2*. *Genes Dev.* **13**, 259-269.

Saijoh, Y., Adachi, H., Sakuma, R., Yeo, C. Y., Yashiro, K., Watanabe, M., Hashiguchi, H., Mochida, K., Ohishi, S., Kawabata, M. et al. (2000). Left-right asymmetric expression of lefty2 and nodal is induced by a signaling pathway that includes the transcription factor FAST2 *Mol. Cell* **5**, 35-47.

Sampath, K., Cheng, A. M., Frisch, A. and Wright, C. V. (1997). Functional differences among Xenopus nodal-related genes in left-right axis determination. *Development* **124**, 3293-3302.

Sasaki, H. and Hogan, B. L. M. (1996). Enhancer analysis of the mouse HNF-3 beta gene: regulatory elements for node/notochord and floor plate are independent and consist of multiple sub-elements. *Genes Cells* **1**, 59-72.

Schier, A. F. and Shen, M. M. (2000). Nodal signalling in vertebrate development. *Nature* **403**, 385-389.

Shawlot, W. and Behringer, R. R. (1995). Requirement for Lim1 in head-organizer function. *Nature* **374**, 425-430.

Shiratori, H., Sakuma, R., Watanabe, M., Hashiguchi, H., Mochida, K., Sakai, Y., Nishino, J., Saijoh, Y., Whitman, M. and Hamada, H. (2001). Two-step regulation of left-right asymmetric expression of Pitx2: initiation by nodal signaling and maintenance by Nkx2. *Mol. Cell* **7**, 137-149.

Sirotkin, H. I., Gates, M. A., Kelly, P. D., Schier, A. F. and Talbot, W. S. (2000). Fast1 is required for the development of dorsal axial structures in zebrafish. *Curr. Biol.* **10**, 1051-1054.

Tam, P. P. L. and Beddington, R. S. P. (1992). Establishment and organization of germ layers in the gastrulating mouse embryo. *Ciba Found. Symp.* **165**, 27-49.

Thomas, P. and Beddington, R. (1996). Anterior primitive endoderm may be responsible for patterning the anterior neural plate in the mouse embryo. *Curr. Biol.* **6**, 1487-1496.

Thomas, P. Q., Brown, A. and Beddington, R. S. P. (1998). Hex: a homeobox gene revealing peri-implantation asymmetry in the mouse embryo and an early transient marker of endothelial cell precursors. *Development* **125**, 85-94.

Tremblay, K. D., Hoodless, P. A., Bikoff, E. K. and Robertson, E. J. (2000). Formation of the definitive endoderm in mouse is a Smad2-dependent process. *Development* **127**, 3079-3090.

Varlet, I., Collignon, J. and Robertson, E. J. (1997). *Nodal* expression in the primitive endoderm is required for specification of the anterior axis during mouse gastrulation. *Development* **124**, 1033-1044.

Waldrip, W. R., Bikoff, E. K., Hoodless, P. A., Wrana, J. L. and Robertson, E. J. (1998). Smad2 signaling in extraembryonic tissues determines anterior-posterior polarity of the early mouse embryo. *Cell* **92**, 797-808.

Whitman, M. (2001). Nodal signaling in early vertebrate embryos. Themes and variations. *Dev. Cell* **1**, 605-617.

Winnier, G., Blessing, M., Labosky, P. A. and Hogan, B. L. M. (1995). Bone Morphogenetic Protein-4 (BMP-4) is required for mesoderm formation and patterning in the mouse. *Genes Dev.* **9**, 2105-2116

Wotton, D. and Massague, J. (2001). Smad transcriptional corepressors in TGF beta family signaling. *Curr. Top. Microbiol. Immunol.* **254**, 145-164.

Yamamoto, M., Meno, C., Sakai, Y., Shiratori, H., Mochida, K., Ikawa, Y., Saijoh, Y. and Hamada, H. (2001). The transcription factor FoxH1 (FAST) mediates Nodal signaling during anterior-posterior patterning and node formation in the mouse. *Genes Dev.* **15**, 1242-1256.

Yan, Y. T., Gritsman, K., Ding, J., Burdine, R. D., Corrales, J. D., Price, S. M., Talbot, W. S., Schier, A. F. and Shen, M. M. (1999). Conserved requirement for EGF-CFC genes in vertebrate left-right axis formation. *Genes Dev.* **13**, 2527-2537.

Zhou, X., Sasaki, H., Lowe, L., Hogan, B. L. M. and Kuehn, M. R. (1993). Nodal is a novel TGF-β-like gene expressed in the mouse node during gastrulation. *Nature* **361**, 543-547.